Inorg. Chem. **2007**, *46*, 1718–1726

Better Understanding of the Species with the Shortest Re_2^{6+} Bonds and Related Re_2^{7+} Species with Tetraguanidinate Paddlewheel Structures

F. Albert Cotton,*,‡ Naresh S. Dalal,*,† Penglin Huang,‡ Sergey A. Ibragimov,‡ Carlos A. Murillo,*,‡ Paula M. B. Piccoli,§ Chris M. Ramsey,† Arthur J. Schultz,§ Xiaoping Wang[||],‡ and Qinliang Zhao‡

Department of Chemistry and Laboratory of Molecular Structure and Bonding, P.O. Box 30012, Texas A&M University, College Station, Texas 77842-3012, Department of Chemistry and Biochemistry and Center for Magnetic Resonance, National High Magnetic Field Laboratory, Florida State University, Tallahassee, Florida 32306-4390, and Intense Pulsed Neutron Source, Argonne National Laboratory, Argonne, Illinois 60439

Received December 5, 2006

A series of compounds has been made containing quadruply bonded $Re_2(hpp)_4X_2$ species (hpp = the anion of 1,3,4,6,7,8-hexahydro-2*H*-pyrimido[1,2*a*]pyrimidine), where X is CF_3SO_3 (**1**), CF_3CO_2 (**2**), and F (**3**). The distances of 2.1562(7), 2.1711(5), and 2.1959(4) Å for **1**–**3** show significant effects of the σ and π electron donating ability of the axial ligands on the metal–metal distance. With the weakly coordinating triflate ligand the Re–Re distance is the shortest for any quadruple bonded species known. In addition to examining the effects of axial ligands on the $Re_2(hpp)_4^{2+}$ core, our study of the $Re_2(hpp)_4^{3+}$ core is being extended beyond the preliminary results previously reported in only one compound $[Re_2(hpp)_4Cl_2]PF_6$ (*Dalton Trans.* **2003**, 1218). We now report the structural characterization by both X-ray and neutron diffraction of the compound $[Re_2(hpp)_4F](TFPB)_2$, **4** (TFPB = the anion tetrakis[3,5-bis(trifluoromethyl)phenyl]borate), and a detailed study by EPR spectroscopy of $[Re_2(hpp)_4Cl_2]PF_6$ at 9.5, 34.5, and 95 GHz frequencies, using dilute fluid solutions, frozen glass, and neat powder, show that the unpaired electron in the $[Re_2(hpp)_4Cl_2]^+$ ion is in an MO of predominant metal character with little mixing from the guanidinate ligands.

Introduction

Guanidinate ligands with a bidentate CN_3 core have attracted much attention because of their strong electron donating ability.[1] Whereas such ligands have frequently been used to stabilize mononuclear compounds,[2] many of which are used as polymerization catalysts,[3] our chief interest has been in the bicyclic guanidinate ligand hpp (hpp = the anion 1,3,4,6,7,8-hexahydro-2*H*-pyrimido[1,2*a*]pyrimidine), that has shown itself to be especially useful in stabilizing dimetal units, M_2^{n+}, such as V_2^{4+},[4] Nb_2^{4+},[5] Cr_2^{4+},[4] $Mo_2^{4+,5+,6+}$,[6] $W_2^{4+,5+,6+}$,[7] Re_2^{6+},[8] Re_2^{7+},[9] Ru_2^{6+},[10] $Os_2^{6+,7+}$,[11] Ni_2^{5+},[12] Pd_2^{6+},[13] and Pt_2^{6+}.[7] The homologous molecules $Mo_2(hpp)_4$ and $W_2(hpp)_4$ are important because of their low ionization energies, the latter being the most easily ionized molecule known.[14]

It should be noted that the strong electron donating ability of the bicyclic hpp ligand is not the only important factor in its stabilizing effect on dimetal units with high oxidation numbers. Thus, while the noncyclic triphenylguanidinate anion can be used to bridge Mo_2^{4+} units, and the basicity of the ligand allows stabilization of Mo_2^{5+} and even the rare Mo_2^{6+} core,[15] the electrode potential for the $Mo_2^{5+/4+}$ process in $Mo_2[(PhN)_2CNHPh]_4$ is about 1.2 V more positive than

* To whom correspondence should be addressed. E-mail: cotton@tamu.edu (F.A.C.), dalal@chemmail.chem.fsu.edu (N.S.D.), murillo@tamu.edu (C.A.M.).
‡ Texas A&M University.
† Florida State University.
§ Argonne National Laboratory.
|| Present address: Department of Chemistry, P.O. Box 305070, University of North Texas, Denton, TX 76203.

(1) Bailey, P. J.; Pace, S. *Coord. Chem. Rev.* **2001**, *214*, 91.

(2) See, for example: (a) Foley, S. R.; Yap, G. P. A.; Richeson, D. S. *Polyhedron*, **2002**, *21*, 619. (b) Soria, D. B.; Grundy, J.; Coles, M. P.; Hitchcock, P. B. *J. Organomet. Chem.* **2005**, *690*, 2315. (c) Coles, M. P.; Hitchcock, P. B. *Organometallics* **2003**, *22*, 5201. (d) Coles, M. P.; Hitchcock, P. B. *Dalton Trans.* **2001**, 1169. (e) Coles, M. P.; Hitchcock, P. B. *Inorg. Chim. Acta* **2004**, *357*, 4330. (f) Oakley, S. H.; Coles, M. P.; Hitchcock, P. B. *Inorg. Chem.* **2004**, *43*, 7564. (g) Coles, M. P.; Hitchcock, P. B. *Eur. J. Inorg. Chem.* **2004**, 2662. (h) Irwin, M. D.; Abdou, H. E.; Mohamed, A. A.; Fackler, J. P., Jr. *Chem. Commun.* **2003**, 2882. (i) Feil, F.; Harder, S. *Eur. J. Inorg. Chem.* **2005**, 4438. (j) Wilder, C. B.; Reitfort, L. L.; Abboud, K. A.; McElwee-White, L. *Inorg. Chem.* **2006**, *45*, 263. (k) Rische, D.; Baunemann, A.; Winter, M.; Fischer, R. A. *Inorg. Chem.* **2006**, *45*, 269.

10.1021/ic062319b CCC: $37.00
Published on Web 01/23/2007

for $Mo_2(hpp)_4$.[16] It has been established that strong interactions of the $p\pi$ orbitals of hpp with the δ orbitals of quadruply bonded species such as Mo_2^{4+} and W_2^{4+} units are also of key importance in lowering the ionization energy of compounds such as $W_2(hpp)_4$.[14]

A well-known group of paddlewheel compounds is that with the formula $M_2(hpp)_4Cl_2$,[17] but relatively few analogues with different axial ligands have been characterized for any given M. It was only recently reported that in the series of triply bonded compounds of the type $W_2(hpp)_4X_2$, X = Cl, PF_6, and TFPB (TFPB = tetrakis[3,5-bis(trifluoromethyl)-phenyl]borate), the anion has an important influence on the W−W distance. This is true even though in each case the anions are very far from the W atoms (the W···Cl separation is more than 3.0 Å).[18] For these compounds, the W−W bond distance decreases from 2.2497(8) Å in $W_2(hpp)_4Cl_2$ to 2.2083(7) Å in $[W_2(hpp)_4](PF_6)_2$ and 2.1920(3) Å in $[W_2(hpp)_4](TFPB)_2$. Calculations at the DFT level suggested that even at long distances, perturbations of metal−metal σ and π interactions by $p\sigma$ and $p\pi$ orbitals of the axial ions are responsible for such variations in W−W bond distances.[19]

These results prompted us to undertake a study of analogous compounds containing quadruply bonded $Re_2(hpp)_4X_2$ species, where X is CF_3SO_3 (**1**), CF_3CO_2 (**2**), and F (**3**) and compare the Re−Re distances to that having X = Cl.[8] The ligands were chosen to cover a range of σ and π electron donating ability. Since rhenium has proven useful in areas such as catalysis,[20] thin film deposition,[21] and building of supramolecules,[22] understanding the sensitivity of the electronic structure in dirhenium compounds to the axial interactions is of importance.

In addition to examining the effects of axial ligands on the $Re_2(hpp)_4^{2+}$ core, our study of the $Re_2(hpp)_4^{3+}$ core is being extended beyond the preliminary results previously reported[9] in only one compound $[Re_2(hpp)_4Cl_2]PF_6$. We now report the structural characterization by both X-ray and neutron diffraction of the compound $[Re_2(hpp)_4F](TFPB)_2$, **4**, and a detailed study by EPR spectroscopy of $[Re_2(hpp)_4Cl_2]PF_6$ at 9.5, 34.5, and 95 GHz frequencies, using dilute solution, frozen glass, and neat powder samples. In particular, this study shows how the combined study of frozen glass and fluid solution provides critically important data for measuring the *s*, *p*, and *d* character of an unpaired electron in metal-based MO.

Results and Discussion

Syntheses. Compounds $Re_2(hpp)_4(CF_3CO_2)_2$ and $Re_2(hpp)_4(CF_3SO_3)_2$ were prepared according to eqs 1 and 2, respectively.

$$Re_2(hpp)_4Cl_2 + 2TlCF_3CO_2 \rightarrow Re_2(hpp)_4(CF_3CO_2)_2 + 2TlCl \quad (1)$$

$$Re_2(hpp)_4Cl_2 + 2TlCF_3SO_3 \rightarrow Re_2(hpp)_4(CF_3SO_3)_2 + 2TlCl \quad (2)$$

These reactions are convenient because TlCl is insoluble in organic solvents such as CH_2Cl_2 and precipitates as a fine white powder that is easily removed by filtration with the aid of Celite. Precipitation of TlCl also helps in driving the reactions to the right thus increasing the yields. The synthesis of $Re_2(hpp)_4F_2$ was performed by fluorination of $Re_2(hpp)_4(CF_3SO_3)_2$ with $[(CH_3)_2N]_3S[(CH_3)_3SiF_2]$. The F anion easily replaces the weakly coordinating triflate anion.

The oxidized compound **4** was made using a two-step process. The first step resembles those in eqs 1 and 2 except for the use of the potassium salt K(TFPB) instead of the corresponding thallium salt. This process produced KCl as

(3) See for example: (a) Zhou, L.; Yao, Y.; Zhang, Y.; Xue, M.; Chen, J.; Shen, Q. *Eur. J. Inorg. Chem.* **2004**, 2167. (b) Duncan, A. P.; Mullins, S. M.; Arnold, J.; Bergman, R. G. *Organometallics* **2001**, *20*, 1808. (c) Giesbrecht, G. R.; Whitener, G. D.; Arnold, J. *Dalton Trans.* **2001**, 923. (d) Gómez, R.; Duchateu, R.; Chernega, A. N.; Teuben, J. H.; Edelmann, F. T.; Green, M. L. H. *J. Organomet. Chem.* **1995**, *491*, 153. (e) Coles, M. P.; Jordan, R. F. *J. Am. Chem. Soc.* **1997**, *119*, 8125. (f) Simoni, D.; Rossi, M.; Rondanin, R.; Mazzali, A.; Baruchello, R.; Malagutti, C.; Roberti, M.; Invidiata, F. P. *Org. Lett.* **2000**, *2*, 3765.

(4) Cotton, F. A.; Timmons, D. J. *Polyhedron* **1998**, *17*, 179.

(5) Cotton, F. A.; Matonic, J. H.; Murillo, C. A. *J. Am. Chem. Soc.* **1997**, *119*, 7889.

(6) Cotton, F. A.; Daniels, L. M.; Murillo, C. A.; Timmons, D. J.; Wilkinson, C. C. *J. Am. Chem. Soc.* **2002**, *124*, 9249.

(7) (a) Clérac, R.; Cotton, F. A.; Daniels, L. M.; Donahue, J. P.; Murillo, C. A.; Timmons, D. J. *Inorg. Chem.* **2000**, *39*, 2581. (b) Cotton, F. A.; Huang, P.; Murillo, C. A.; Timmons, D. J. *Inorg. Chem. Commun.* **2002**, *5*, 501. (c) Cotton, F. A.; Huang, P.; Murillo, C. A.; Wang, X. *Inorg. Chem. Commun.* **2003**, *6*, 121.

(8) Cotton, F. A.; Gu, J.; Murillo, C. A.; Timmons, D. J. *J. Chem. Soc., Dalton Trans.* **1999**, 3741.

(9) Berry, J. F.; Cotton, F. A.; Huang, P.; Murillo, C. A. *Dalton Trans.* **2003**, 1218.

(10) Bear, J. L.; Li, Y.; Han, B.; Kadish, K. M. *Inorg. Chem.* **1996**, *35*, 1395.

(11) Cotton, F. A .; Dalal, N. S.; Huang, P.; Murillo, C. A.; Stowe, A. C.; Wang, X. *Inorg. Chem.* **2003**, *42*, 670.

(12) Berry, J. F.; Cotton, F.A.; Huang, P.; Murillo, C. A.; Wang, X. *Dalton Trans.* **2005**, 3713.

(13) Cotton, F. A.; Gu, J.; Murillo, C. A.; Timmons, D. J. *J. Am. Chem. Soc.* **1998**, *120*, 13280.

(14) Cotton, F. A.; Gruhn, N. E.; Gu, J.; Huang, P.; Lichtenberger, D. L.; Murillo, C. A.; Van Dorn, L. O.; Wilkinson, C. C. *Science* **2002**, *298*, 1971.

(15) (a) Bailey, P. J.; Bone, S. F.; Mitchell, L. A.; Parsons, S.; Taylor, K. J.; Yellowlees, L. J. *Inorg. Chem.* **1997**, *36*, 867. (b) Bailey, P. J.; Bone, S. F.; Mitchell, L. A.; Parsons, S.; Taylor, K. J.; Yellowlees, L. J. *Inorg. Chem.* **1997**, *36*, 5420.

(16) Cotton, F. A.; Daniels, L. M.; Murillo, C. A.; Timmons, D. J.; Wilkinson, C. C. *J. Am. Chem. Soc.* **2002**, *124*, 9249.

(17) Cotton, F. A.; Murillo, C. A.; Wang, X.; Wilkinson, C. C. *Inorg. Chim. Acta* **2003**, *351*, 183 and references therein.

(18) Cotton, F. A.; Donahue, J. P.; Gruhn, N. E.; Lichtenberger, L.; Murillo, C. A.; Timmons, D. J.; Van Dorn, L. O.; Villagrán, D.; Wang, X. *Inorg. Chem.* **2006**, *45*, 201.

(19) More recently, calculations on the $Pd_2(carboxylate)_2(orthometalatated\ phosphine)_2Cl_2$ system also suggest an important effect of the axial ligands on the Pd—Pd distance. See: Cotton, F. A.; Koshevoy, I. O.; Lahuerta, P.; Murillo, C. A.; Sanaú, M.; Ubeda, M. A.; Zhao, Q. *J. Am. Chem. Soc.* **2006**, *128*, 13674.

(20) (a) Balandin, A. A.; Karpeiskaya, E. I.; Tolstopyatova, A. A. *Z. Fiz. Khim.* **1959**, *33*, 2471. (b) Balandin, A. A.; Karpeiskaya, E. I.; Tolstopyatova, A. A. *Dokl. Akad. Nauk SSSR* **1958**, *122*, 227.

(21) (a) Despotuli, A. L.; Matveeva, L. A.; Despotuli, L. A. *Ionics* **1998**, *4*, 383. (b) Yamasaki, H.; Suzuki, K.; Guidotti, E.; Mosca, E.; Leusink, G.; Kawano, Yu.; Mcfeely, F. R.; Malhotra, S. G. *U.S. Pat. Appl. Publ.* **2006**, 11. (c) Lungu, C. P.; Mustata, I.; Musa, G.; Lungu, A. M.; Zaroschi, V.; Iwasaki, K.; Tanaka, R.; Matsumura, Y.; Iwanaga, I.; Tanaka, H.; Oi, T.; Fujita, K. *Surf. Coat. Technol.* **2005**, *200*, 399. (d) Reddy, V. R. *Mat. Chem. Phys.* **2005**, *93*, 286.

(22) (a) Mondal, A.; Sarkar, S.; Chopra, D.; Rajak, K. K. *Inorg. Chim. Acta* **2006**, *359*, 2141. (b) Reger, D. L.; Brown, K. J.; Smith, M. D. *J. Organomet. Chem.* **2002**, *658*, 50.

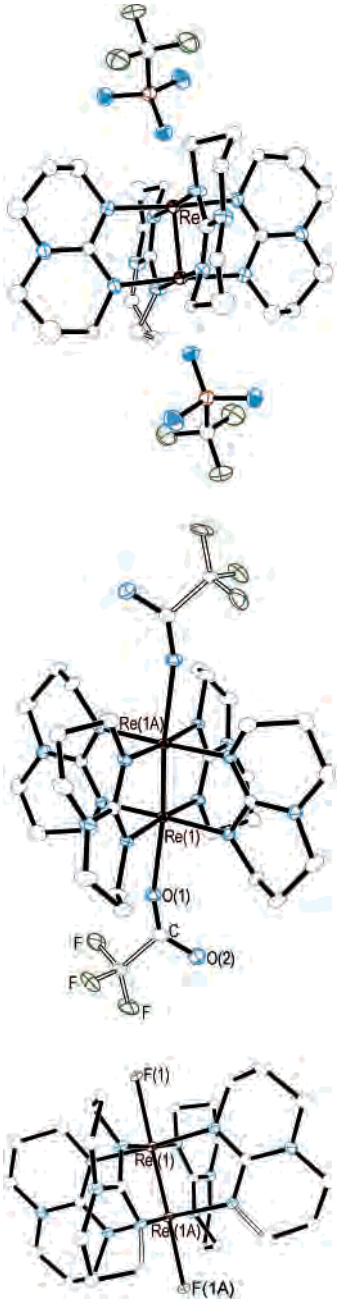

Figure 1. Structures of the Re_2^{6+} paddlewheel compounds **1** (top), **2** (center), and **3** (bottom). Displacement ellipsoids are drawn at the 30% probability level. Color code: red for Re, blue for N, purple for O, green for F, orange for S, and gray for C atoms.

a white solid and $[Re_2(hpp)_4](TFPB)_2$. Addition of 2 equiv[23] of oxidizing agent $[Ag(CH_3CN)_2]PF_6$ generated $[Re_2(hpp)_4F](TFPB)_2$ (vide infra). In this reaction, the silver compound acts not only as an oxidizing but also as a fluorine source. Although decomposition of PF_6^- and other fluorinated anions such as BF_4^- is not generally expected, it has been observed before.[24]

(23) The use of 2 equiv of $[Ag(CH_3CN)_2]PF_6$ was with the intention of generating an Re_2^{8+} species that had been observed in the cyclovoltammogram of $Re_2(hpp)_4Cl_2$ done using NBu_4PF_6 as electrolyte. See ref 9. However, only the singly oxidized species **4** was isolated from this reaction.

(24) See, for example: Clérac, R.; Cotton, F. A.; Daniels, L. M.; Dunbar, K. R.; Murillo, C. A.; Pascual, I. *Inorg. Chem.* **2000**, *39*, 752.

Table 1. Selected Interatomic Distances[a] for **1**, **2**·$2CH_2Cl_2$, **3**·$3CH_2Cl_2$, and $Re_2(hpp)_4Cl_2$

compound	Re−Re (Å)	Re−X_{ax} (Å)	Re−N (Å)	ref
$Re_2(hpp)_4(CF_3SO_3)_2$, **1**	2.1562(7)	2.484(5)	2.079[8]	this work
$Re_2(hpp)_4(CF_3CO_2)_2$, **2**	2.1711(5)	2.408(2)	2.080[6]	this work
$Re_2(hpp)_4F_2$, **3**	2.1959(4)	2.209(2)	2.078[2]	this work
$Re_2(hpp)_4Cl_2$	2.189(2)	2.749(5)	2.070[7]	8

[a] Numbers in square brackets apply to average values.

Crystal Structures of 1−3. These structures are shown in Figure 1. The triflate, trifluoroacetate, and fluoride ligands are located in axial positions of a paddlewheel having the $Re_2(hpp)_4^{2+}$ core. All three molecules possess a crystallographic inversion center at the midpoint of each Re−Re bond. The ring conformation of the hpp ligands is disordered in all the molecules.[25] As shown in Table 1, the Re−Re distances are 2.1562(7), 2.1711(5), and 2.1959(4) Å for **1**−**3**. These distances are short when compared to those of other quadruply bonded Re_2^{6+} compounds.[26] The Re−Re distance in **1** is shorter by ca. 0.02 Å than those in $Li_2Re_2(CH_3)_8 \cdot Et_2O$,[27] $Re_2(O_2CCH_3)_2(CH_3)_2(\eta^1\text{-}O_2CCH_3)$,[28] $Re_2[(PhN)_2CPh]_2Cl_4$,[29] and $Re_2[(PhN)_2CH]_2Cl_4$,[30] which have the shortest Re−Re distances previously reported for Re_2^{6+} compounds (about 2.177 Å), and it is therefore now the shortest one known. The longest Re−X_{ax} distance of 2.484(5) Å is also found in **1** which has the shortest Re−Re distance. Conversely, the shortest Re−X_{ax} distance (2.209(2) Å) is found in **3**, the species that contains strongly coordinating fluoride anions and the longest Re−Re distance in the three new $Re_2(hpp)_4^{2+}$ compounds. The Re−O distances in **1** are considerably longer than those in other Re_2^{6+} species with axially coordinated anions containing O-donor atoms, e.g., 2.18(3) Å in $[Re_2(n\text{-}C_3H_7CO_2)_4](ReO_4)_2$.[31] The data in Table 1 indicate that as the interaction between the axial ligand and the rhenium atoms increases, there is an increase in the metal−metal bond distance which reduces the Re−Re interaction. This is parallel to the results in $W_2(hpp)_4X_2$ compounds.[18]

Structural Characterization of 4. An initial X-ray structure showed the existence of a paddlewheel structure with four somewhat conformationally disordered hpp ligands[32] and two weakly diffracting axial ligands. The terminal ligands on the Re atoms in the paddlewheel complex were suspected to be F, but the possibility of their being OH^- or H_2O[33] could not be ruled out by conventional spectroscopy.

(25) Disorder of hpp ligands in paddlewheel compounds is common, but the disorder is generally well understood. See, for example, ref 17.

(26) Walton, R. A. In *Multiple Bonds Between Metal Atoms*; Cotton, F. A., Murillo, C. A., Walton, R. A., Eds.; Springer Science and Business Media, Inc.: New York, 2005; Chapter 8.

(27) Cotton, F. A.; Gage, L. D.; Mertis, K.; Shive, L. W.; Wilkinson, G. *J. Am. Chem. Soc.* **1976**, *98*, 6922.

(28) Hursthouse, M. B.; Abdul Malik, K. M. *J. Chem. Soc., Dalton Trans.* **1979**, 409.

(29) Cotton, F. A.; Shive, L. W. *Inorg. Chem.* **1975**, *14*, 2027.

(30) Cotton, F. A.; Daniels, L. M.; Haefner, S. C. *Inorg. Chim. Acta* **1999**, *285*, 149.

(31) Calvo, C.; Jayadevan, N. C.; Lock, C. J. L.; Restivo, R. *Can. J. Chem.* **1970**, *48*, 219.

(32) As mentioned in ref 25, disorder of hpp ligands is common.

(33) Because the Re−X axial was about 2.03 Å, an oxide group could be ruled out because Re−O distances would be expected to be significantly shorter.

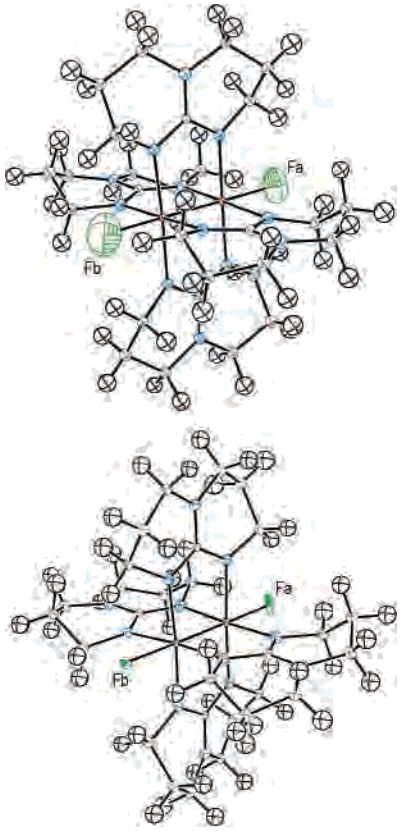

Figure 2. The structure from neutron diffraction of the cation in **4** after isotropic refinement of the structure and fluorine atoms Fa and Fb refined anisotropically with full occupancy (top) and using fractional occupancies of 0.62(2) for Fa and 0.42(2) for Fb (bottom). Note the good match in the size of the displacement ellipsoids in the bottom view. Displacement ellipsoids are plotted at 50% probability with rhenium in red, nitrogen in blue, carbon in gray, fluorine in green, and hydrogen in black.

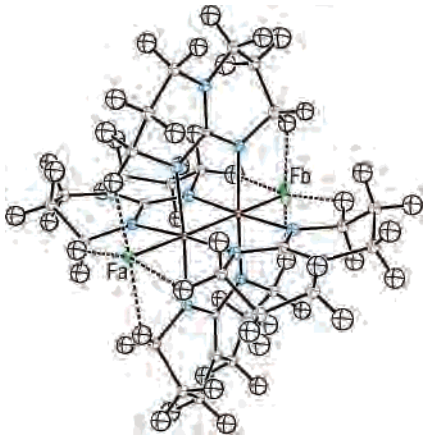

Figure 3. ORTEP of the cation in **4** showing close C−H···F contacts (dashed lines).

To resolve this uncertainty, neutron diffraction was performed on this complex to confirm or exclude the possibility of an H atom on the axial ligand. It should be noted that the nature of the terminal ligand could affect the assignment of the oxidation state of the dirhenium core.

The results from neutron data were generally consistent with those from X-ray diffraction data. When the scattering in the region of the axial atoms was examined carefully and hydrogen atoms on the axial ligands, labeled as H3A and H3B, were inserted simulating OH^- groups, structure factor

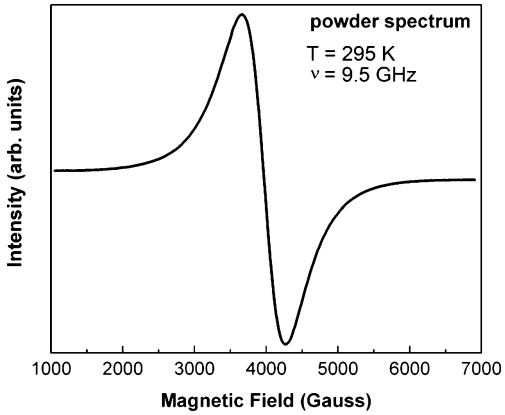

Figure 4. X-band EPR spectrum of a powder of $[Re_2(hpp)_4Cl_2]PF_6$.

calculations resulted in a higher *Rw* value (0.133) and negative scattering density around the positions of the hydrogen atoms, as seen in Figure S1. However, negative scattering density was absent when the axial atoms were refined as F atoms (Figure S2). This led with certainty to the conclusion that the terminal ligands on Re1 and Re2 are not OH^- but F^- ligands. Fluorine atoms were placed at these sites and refined accordingly, as shown on the top image of Figure 2.

However, examination of the isotropic thermal parameters for the structure revealed that with full occupancy for the terminal F ligands, the U_{iso} values were far larger than comparable atoms in the structure, even the fluorine atoms in the TFPB anions (not pictured in Figure 2). Even more unusual was the fact that the values exceeded those found for the hydrogen atoms of the structure, also refined with isotopic thermal parameters. These terminal fluorine ligands were then refined anisotropically for a closer examination (see lower image in Figure 2). Refinement of the fractional occupancies for these terminal F ligands resulted in fractional occupancy values of approximately 0.62(2) for Fa and 0.42(2) for Fb. These results suggest that there is only one terminal F ligand disordered over the two crystallographically independent terminal sites of the dinuclear species. This results in a chemical formula $[Re_2(hpp)_4F](TFPB)_2$ with a Re_2^{7+} core. It should be noted that paddlewheel compounds with an M_2^{7+} core are rare; the only other known compounds that have been structurally characterized are the homologous $[M_2(hpp)_4Cl_2]PF_6$ species, M = Re[9] and Os.[11]

When a similar model was used for the X-ray data, refinement proceeded smoothly, and the results were consistent, varying by no more than a few standard deviations, as shown in Table 2.[34] The core structure for the cation in **4**, as determined from X-ray data, is given in Figure S3. The displacement ellipsoids do not show any unusual features. In this compound, the Re_2^{7+} species has a formal bond order of 3.5, and the Re−Re distance (2.1874(3) Å from X-ray data or 2.186(4) Å from neutron data) is longer than those in the quadruply bonded compounds **1** and **2** but

(34) The only significant difference was that for the X-ray structure the occupancy values for each Fa and Fb refined to 0.48(1). The difference is attributed to the temperatures used for each data collection, 40 K for the neutron data, and 213 K for the X-ray data.

Table 2. Selected Bond Distances (Å) and Angles (deg) for the Cation in **4** from X-ray and Neutron Diffraction Data

atoms	distance X-ray	neutron	atoms	distance X-ray	neutron
Re1−Re2	2.1875(3)	2.186(4)	Re2−N23	2.049(5)	2.046(4)
Re1−Fa	2.038(6)	2.021(9)	Re2−N33	2.036(4)	2.060(4)
Re2−Fb	2.027(6)	2.040(11)	Fa−H2A		2.147(12)
Re1−N1	2.036(5)	2.049(4)	Fa−H12A		2.185(12)
Re1−N11	2.047(5)	2.051(4)	Fa−H22A		2.208(12)
Re1−N21	2.047(5)	2.060(4)	Fa−H32B		2.166(12)
Re1−N31	2.041(5)	2.049(4)	Fb−H7A		2.087(13)
Re2−N3	2.047(5)	2.049(4)	Fb−H17A		2.121(13)
Re2−N13	2.032(5)	2.030(4)	Fb−H27A		2.184(13)
			Fb−H37B		2.211(13)

atoms	angle X-ray	neutron	atoms	angle X-ray	neutron
FA−Re1−N1	87.4(2)	87.91(27)	N3−Re2−N13	89.4(2)	90.04(15)
FA−Re1−N11	88.3(2)	88.59(29)	N3−Re2−N23	176.7(2)	175.22(18)
FA−Re1−N21	89.1(2)	89.46(26)	N3−Re2−N33	89.4(2)	88.30(14)
FA−Re1−N31	88.7(2)	88.88(29)	N13−Re2−N23	91.8(2)	92.33(15)
N1−Re1−N11	89.5(2)	89.32(15)	N13−Re2−N33	176.1(2)	175.59(18)
N1−Re1−N21	176.2(2)	176.79(18)	N23−Re2−N33	89.2(2)	89.03(15)
N1−Re1−N31	91.0(2)	91.99(15)	Fa−H2A−C2		124.0(7)
N11−Re1−N21	89.1(2)	88.77(15)	Fa−H12A−C12		122.4(7)
N11−Re1−N31	177.0(2)	177.10(18)	Fa−H22A−C22		120.7(7)
N21−Re1−N31	90.3(2)	89.80(15)	Fa−H32B−C32		122.8(7)
Fb−Re2−N3	89.1(2)	87.26(31)	Fb−H7A−C7		126.4(7)
Fb−Re2−N13	88.7(2)	88.12(32)	Fb−H17A−C17		126.1(7)
Fb−Re2−N23	87.9(2)	88.67(31)	Fb−H27A−C27		119.6(7)
Fb−Re2−N33	87.6(2)	87.71(32)	Fb−H37B−C37		120.1(7)

Table 3. Bond Distances (Å) and Angles (deg) for Hydrogen Atoms Involved in Short C−H···F Contacts in **4**[a]

atoms	distance/ angle	atoms	distance/ angle
H2A−C2	***1.066(11)***	***H22A−C22***	***1.099(11)***
H2B−*C*2	1.098(10)	H22B−C22	1.108(10)
H2A−C2−H2B	107.5(7)	H22A−C22−H22B	107.4(7)
H7A−C7	***1.091(11)***	***H27A−C27***	***1.091(10)***
H7B−C7	1.102(10)	H27B−C27	1.111(10)
H7A−C7−H7B	107.1(7)	H27A−C27−H27B	106.9(7)
H12A−C12	***1.078(10)***	H32A−C32	1.099(10)
H12B−C12	1.115(10)	***H32B−C32***	***1.109(11)***
H12A−C12−H12B	108.9(7)	H32A−C32−H32B	106.2(7)
H17A−C17	***1.078(11)***	H37A−C37	1.081(10)
H17B−C17	1.117(11)	***H37B−C37***	***1.063(10)***
H17A−C17−H17B	106.5(7)	H37A−C37−H37B	108.7(7)

[a] Values for hydrogen atoms involved in the short contact are in bold/italics. The average C−H bond for the hpp ligand in this structure is 1.094(3) Å, and the average angle is 107.3(3)°.

slightly shorter than those in **3** and $Re_2(hpp)_4Cl_2$. This Re−Re distance of 2.1874(3) Å in **4** is significantly shorter than that in the other Re_2^{7+} species known, namely $[Re_2(hpp)_4Cl_2]PF_6$,[9] which has an Re−Re distance of 2.2241(4) Å. The difference is attributable to the presence of only one axial ligand (disordered over two positions) in **4**, while there are two axially coordinated Cl^- groups in $Re_2(hpp)_4Cl_2$.

Because hydrogen atoms are accurately located from neutron diffraction data, it is of interest to note the arrangement of hydrogen atoms around the terminal ligands Fa and Fb. This arrangement is shown in Figure 3, and bond distances and angles around Fa and Fb are listed in Table 2. The C−H···F distances, at 2.08−2.21 Å, are far less than the sum of van der Waals radii (2.67 Å)[35] but also less than that found for typical C−H···F−C contacts.[36] The short contacts listed in Table 3 show that the general trend is for the hydrogen atom involved in the short contact to also have a shorter distance to the carbon atom it is bound to than does the other hydrogen atom in the same methylene group; H32B is the only exception to this. Comparisons of the methylene groups in the hpp ligands do not suggest that the parameters listed in Table 3 are unusual; the average C−H bond for the hpp ligand in this structure is 1.094(3) Å, and the average angle is 107.3(3)°. The C−H bonds do not appear to be influenced by the presence of the terminal F ligands, and so the short H···F contacts are most likely directed by the geometry of the ligands in the paddlewheel species.

EPR Spectroscopy of $[Re_2(hpp)_4Cl_2]PF_6$. Because of the Re_2^{7+} core, **4** is paramagnetic. Multifrequency/variable temperature EPR experiments were carried out to assist in the characterization of the bulk magnetic properties and electronic structure. The room-temperature X-band (9.5 GHz) powder spectrum (Figure 4) consists of a single exchange narrowed featureless line at $g = 1.7421$ with a peak-to-peak line width of 600 G. This g-value is in reasonably good agreement with that obtained from the Curie−Weiss fit ($g = 1.696$)[9] to the magnetic susceptibility.

To derive more detailed information and resolve the hyperfine structure, the spectra were also obtained in a 10 mM solution in CH_2Cl_2. The dilution reduced the solid-state effects (dipolar and magnetic exchange) providing a fairly well resolved spectrum as shown in Figure 5. The hyperfine structure arises from the two natural isotopes:[37] ^{185}Re, 37.4% abundance, $g_n = 1.2748$, $I = 5/2$ and ^{187}Re, 62.6% abundance, $g_n = 1.2878$, $I = 5/2$, both having approximately the same hyperfine coupling constants within our experimental resolution, based on the ratio of their nuclear g-values. The

(35) Bondi, A. *J. Phys. Chem.* **1964**, *68*, 441.
(36) Desiraju, G. R. *Acc. Chem. Res.* **2002**, *35*, 565.
(37) (a) Weil, J. A.; Bolton, J. R.; Wertz, J. E. *Electron Paramagnetic Resonance: Elementary Theory and Practical Applications*; John Wiley & Sons: New York, 1994. (b) Morton, J. R.; Preston, K. F. *J. Magn. Reson.* **1978**, *30*, 577. (c) Dalal, N. S.; Millar, J. M.; Jagadeesh, M. S.; Seehra, M. S. *J. Chem. Phys.* **1981**, *74*, 1916.

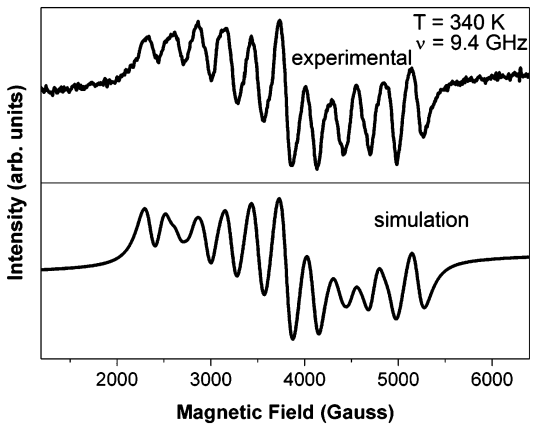

Figure 5. The isotropic solution EPR spectrum of $[Re_2(hpp)_4Cl_2]PF_6$ (10 mM in CH_2Cl_2) consists of 11 hyperfine peaks from coupling with 2 equivalent Re nuclei ($I = 5/2$).

Table 4. EPR Parameters for the Re_2^{7+} Species in $[Re_2(hpp)_4Cl_2]PF_6$

$g_{xx} = 1.8487 \pm 0.0001$	$A_{xx} = 360 \pm 1$ G (931 MHz)
$g_{yy} = 1.7725 \pm 0.0005$	$A_{yy} = 298$ G ± 8 G (739 MHz)
$g_{zz} = 1.6392 \pm 0.0005$	$A_{zz} = 190$ G ± 4 G (436 MHz)
$g_{iso} = 1.7535 \pm 0.0002$	$A_{iso} = 283$ G ± 5 G (695 MHz)
$g_{powder} = 1.7421 \pm 0.0001$	

X-band solution spectrum in Figure 5 was taken using a sealed tube at 340 K. The presence of 11 hyperfine lines indicates that the unpaired spin is coupled to the two equivalent Re ions in the Re_2^{7+} core. The spectrum is not fully isotropic even at elevated temperatures, which may be due to relatively slow tumbling of the heavy molecules with bulky ligands. The simulation (Figure 5, lower panel) reveals $g_{iso} = 1.7535 \pm 0.0002$ and $A_{iso} = 283 \pm 5$ G (695 MHz) (Table 4). The significant deviation from $g = 2$ is due to spin−orbit coupling from the heavy Re ions and indicates that the oxidation is at least partially metal-based.[37]

More detailed information was obtained from frozen glass spectra obtained at 34.5 and 95 GHz, since in general frozen-glass spectra are capable of yielding the full (isotropic + anisotropic) hyperfine tensor. It is important to note that the anisotropic component provides the amount of spin density in the *d*-orbitals (involved in δ-bonding).

A typical Q-band (34.5 GHz) spectrum obtained at 153 K on a frozen CH_2Cl_2 solution is shown in Figure 6. It consists of 33 lines, superimposed on one another to some extent. The spectrum was analyzed by solving the standard spin Hamiltonian

$$\mathcal{H} = \beta_e H \cdot g_e \cdot S + \Sigma I_i \cdot A \cdot S_i - \Sigma g_n \cdot \beta_n H \cdot I_i$$

where the symbols have their usual meaning: H is the Zeeman field, S and I are the electronic and nuclear spins, and A is the hyperfine tensor of the ith nucleus. The frozen glass spectrum was generated using the computer program XSophe supplied by Bruker, that uses second-order perturbation theory on the hyperfine interaction and full powder averaging. This computer-simulated spectrum is at the bottom of Figure 6. The fitting was obtained by utilizing fully anisotropic g and A tensors, and values are given in Table 4. The isotropic value $(A_{xx} + A_{yy} + A_{zz})/3 = 283$ G is in

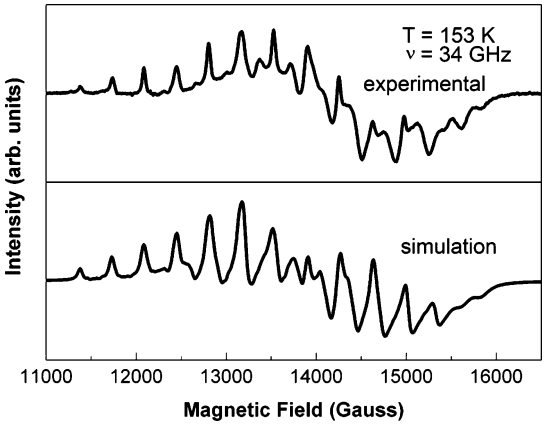

Figure 6. The 33 line frozen glass EPR spectrum of $[Re_2(hpp)_4Cl_2]PF_6$ at 153 K (top) along with simulation (bottom). Relevant parameters are in Table 4.

excellent agreement with the isotropic value from the solution spectrum. The same *g*-tensor and hyperfine tensor parameters agreed with values extracted from the W-band (95 GHz) spectrum. The W-band data are not given here because these spectra were less well resolved, owing to the greater *g*-strain and hence larger line widths at higher Zeeman fields. Because of the large *g*-tensor anisotropy in this compound, the Q-band spectra yielded the optimum combination of spectral resolution and intensity. This emphasizes the value of using multifrequency EPR measurements whenever possible.

The spin density in the *d*-orbitals was obtained by comparing the dipolar part of the hyperfine tensor of the Re nuclei with that theoretically expected from a *d*-electron in the Re 5*d* orbitals. From Table 4, the dipolar contribution can be obtained as the difference between a principal value and the isotropic contribution using the relationship $B_i = A_{iso} - A_{ii}$ for the ith component, where $A_{iso} = 283$ G. In this way, the value of B_x was calculated as $B_x = (283-360)$ Gauss $= -77$ G. Similar calculations give $B_y = -15$ G and $B_z = +93$ G. Using the value of 93 G as the *z*-component of the dipolar tensor, the spin density in the *d*-orbital can be estimated by noting that the theoretical value of the dipolar coupling for an electron in the 5*d* orbital of the Re atom is 23.6 mT or 236 G.[37] This yields a spin density of (93/236) $\times$ 100 = ~40% in the *d*-orbital of a Re atom or a total of ca. 80% for the two rhenium atoms in the Re_2^{7+} unit. While this estimate of the spin density in the δ-bonds might have a significant error associated with it (because of the error in the theoretical value[37] and the utilization of a rather simple model), these results clearly imply that much of the spin density is in the metal *d*-orbitals. Taken together these results establish that the unpaired electron is in a mainly metal-centered MO.

The results from the temperature dependence of the frozen glass spectrum at 34 GHz support the presence of weak antiferromagnetic exchange between dimeric units within the crystal. The intensity of the frozen glass spectrum increases inversely with temperature as expected for simple Curie paramagnets in which no interactions exist between paramagnetic centers. Therefore, it is concluded that the downturn near 10 K in the powder χT plot given in ref 9 is due to

Table 5. Crystallographic Data for **1**, **2**·$2CH_2Cl_2$, **3**·$3CH_2Cl_2$, and **4**

	1	**2**·$2CH_2Cl_2$	**3**·$3CH_2Cl_2$	**4**
formula	$Re_2C_{30}H_{48}F_6N_{12}O_6S_2$	$Re_2C_{34}H_{52}Cl_4F_6N_{12}O_4$	$Re_2C_{31}H_{54}Cl_6F_2N_{12}$	$Re_2C_{92}H_{72}B_2F_{49}N_{12}$
formula weight	1223.32	1321.08	1217.96	2670.64
space group	$P2_1/n$	$P\bar{1}$	$C2/c$	$P\bar{1}$
a (Å)	9.354(2)	9.459(3)	12.760(2)	13.1621(6)
b (Å)	15.419(3)	10.728(4)	15.583(3)	14.8033(7)
c (Å)	13.652(3)	11.194(4)	20.772(4)	26.022(1)
α (deg)	90	93.392(6)	90	87.370(1)
β (deg)	94.440(3)	103.510(5)	92.453(3)	88.908(1)
γ (deg)	90	95.500(6)	90	76.862(1)
V (Å^3)	1963.1(6)	1095.5(6)	4127(1)	4932.1(4)
Z	2	1	4	2
d_{calc} (g cm^{-3})	2.070	2.002	1.960	1.798
μ (Mo Kα) (mm^{-1})	6.355	5.843	6.300	2.598
T (°C)	−60	−60	−60	−60
R1,[a] wR2[b] ($I > 2\sigma(I)$)	0.0392, 0.0976	0.0210, 0.0528	0.0287, 0.0699	0.0410, 0.0919
R1,[a] wR2[b] (all data)	0.0548, 0.1109	0.0223, 0.0536	0.0304, 0.0709	0.0568, 0.1026

[a] $R1 = \Sigma||F_o|-|F_c||/\Sigma|F_o|$. [b] $wR2 = [\Sigma[w(F_o^2 - F_c^2)^2]/\Sigma[w(F_o^2)^2]]^{1/2}$.

dimer-to-dimer antiferromagnetic coupling on the order of $\theta = -0.515$ K, as determined previously.[9]

Concluding Remarks. A series of compounds having the core $Re_2(hpp)_4^{2+}$ with two axial ligands has shown that the σ and π donating ability of the ligand is of great importance in determining the metal−metal distance. As the interaction between the axial ligand and the rhenium atoms increases, there is an increase in the metal−metal bond distance thus reducing the Re−Re interaction. When the axial ligands are the weakly coordinating triflate anions, the Re−Re distance is only 2.1562(7) Å, the shortest for any quadruply bonded species known. The short bond is consistent with DFT calculations reported earlier that showed the stabilization of the Re_2^{6+} core by hpp ligands.[8]

The species $[Re_2(hpp)_4F](TFPB)_2$, containing the rare Re_2^{7+} core, has also been characterized using neutron and X-ray diffraction. A systematic combination of multifrequency (9−95 GHz) and variable temperature (fluid to frozen-glass phase) EPR spectroscopy of the analogous compound $[Re_2(hpp)_4Cl_2]PF_6$ clearly indicates that the unpaired electron in this Re_2^{7+} species resides in a dominantly metal-based orbital.

Experimental Section

General. Operations were routinely carried out under an inert atmosphere in Schlenkware using dry and oxygen-free solvents. The thallium salts $TlCF_3CO_2$ and $TlCF_3SO_3$ were prepared by reaction of 1 equiv of Tl_2CO_3 with 2 equiv of the corresponding acid. The fluorinating reagent tris(dimethylamino)sulfur trimethylsilyl difluoride, $[(CH_3)_2N]_3S[(CH_3)_3SiF_2$, was purchased from Aldrich and used as received. The parent dirhenium compound $Re_2(hpp)_4Cl_2$,[8] $[Re_2(hpp)_4Cl_2]PF_6$,[9] K(TFPB),[38] and $[Ag(CH_3CN)_2]PF_6$[39] were prepared according to literature procedures.

Physical Measurements. ^{1}H NMR spectra were obtained on a Varian XL-300 spectrometer, with chemical shifts (δ, ppm) referenced to the signal of the protonated residue of the deuterated solvent. The IR spectra were recorded on a Bruker TENSOR 27 spectrometer using KBr pellets. Elemental analyses were carried out by Robertson Microlit Laboratory, NJ, using samples dried under vacuum to remove interstitial solvent molecules from the crystals.

Synthesis of $Re_2(hpp)_4(CF_3SO_3)_2$ (1). A mixture of $Re_2(hpp)_4Cl_2$ (100 mg, 0.100 mmol) and $TlCF_3SO_3$ (71 mg, 0.200 mmol) was placed in a flask which was filled with N_2. After addition of 30 mL of CH_2Cl_2, the solution was stirred overnight. The volume of the solution was then reduced to ca. 15 mL and filtered through Celite. A layer of hexanes was added on top of the solution. Formation of purple crystals began within 2 h, and crystallization was complete in 1 week. Yield: 106 mg, 87%. IR (KBr, cm^{-1}): 2957 (w), 2864 (w), 1638 (w), 1539 (vs), 1487 (m), 1445 (m), 1391 (m), 1311 (s), 1228 (s), 1208 (vs), 1169 (m), 1137 (w), 1069 (w), 1015 (s), 803 (w), 757 (vw), 705 (m), 630 (vw), 575 (vw), 518 (vw), 509 (vw), 497 (vw), 474 (vw), 432 (vw). Calcd for $Re_2C_{30}H_{48}N_{12}O_6F_6S_2$: C, 29.46; H, 3.93; N, 13.75%. Found: C, 29.30; H, 3.75; N, 13.51%. ^{1}H NMR ($CDCl_3$, δ): 1.983 (q, $CH_2CH_2CH_2$, 8H), 3.354 (t, $CH_2CH_2CH_2$, 8H), 3.557 (t, $CH_2CH_2CH_2$, 8H).

Synthesis of $Re_2(hpp)_4(CF_3CO_2)_2$ (2). A mixture of $Re_2(hpp)_4Cl_2$ (100 mg, 0.100 mmol) and $TlCF_3CO_2$ (64 mg, 0.200 mmol) was placed in a flask, and the air was removed under vacuum for 30 min. Then 30 mL of CH_2Cl_2 was added to the flask, and the purple solution was stirred overnight. The following day the mixture was heated to reflux and filtered through Celite while still hot. The volume of the purple solution was reduced to a half, and the solution was then layered with hexanes. In 2 h formation of purple crystals began, and crystallization was complete in 1 week. Yield: 92 mg, 80%. IR (KBr, cm^{-1}): 2955 (w), 2856 (w), 1689 (vs), 1535 (s), 1492 (m), 1477 (m), 1448 (m), 1392 (m), 1371 (vw), 1313 (vw), 1286 (m), 1213 (m), 1193 (s), 1134 (s), 1071 (w), 1032 (w), 826 (w), 795 (w), 754 (w), 715 (w), 434 (vw). Calcd for $Re_2C_{32}H_{48}N_{12}O_4F_6$: C, 33.39; H, 4.17; N, 14.61%. Found: C, 33.30; H, 3.94; N, 14.40%. ^{1}H NMR ($CDCl_3$, δ): 1.932 (q, $CH_2CH_2CH_2$, 8H), 3.352 (t, $CH_2CH_2CH_2$, 8H), 3.508 (t, $CH_2CH_2CH_2$, 8H).

Synthesis of $Re_2(hpp)_4F_2$ (3). A solution of **1** (40 mg, 0.030 mmol) and $[(CH_3)_2N]_3SSi(CH_3)_3F_2$ (30 mg, 0.10 mmol) in 15 mL of CH_2Cl_2 was stirred at ambient temperature overnight. After the volume of the mixture was reduced to 10 mL, it was filtered through Celite, and the filtrate was layered with hexanes. Formation of purple crystals began within 2 h, and crystallization was complete in 1 week. Yield: 22 mg, 76%. IR (KBr, cm^{-1}): 3135 (b, w), 2938 (m), 2920 (w), 2831 (m), 1535 (vs), 1505 (s), 1477 (vw), 1454 (m), 1391 (m), 1327 (vw), 1312 (m), 1283 (m), 1252 (vw), 1212 (m), 1140 (m), 1077 (w), 1029 (w), 753 (w), 707 (vw), 426 (vw).

(38) Buschmann, W. E.; Miller, J. S. *Inorg. Synth.* **2002**, *33*, 83.
(39) Iqbal, J.; Sharp, D. W. A.; Winfield, J. M. *J. Chem. Soc., Dalton Trans.* **1989**, 461.

Table 6. Crystal Data and Structure Refinement Parameters for **4** from Neutron Diffraction

formula	$C_{96}H_{78}B_2F_{49}N_{14}Re_2$
formula weight	2733.718
temperature (K)	40(1)
crystal system	*triclinic*
space group	$P\bar{1}$
a (Å)	13.036(2)
b (Å)	14.613(3)
c (Å)	25.751(4)
α (deg)	87.617(14)
β (deg)	88.199(13)
γ (deg)	76.658(13)
V (Å^3)	4767.71094
Z	2
d_{calc} (g cm^{-3})	1.857
crystal size (mm^3)	5 × 1 × 1
radiation	neutrons
data collection technique	time-of-flight Laue
$\mu(\lambda)$ (cm^{-1})	1.023 + 0.992 λ
max, min transmission	0.8259, 0.4040
extinction parameter	1.11(2) × 10^{-5}
d_{min} (Å)	0.7
no. of reflections	17429
no. of reflections ($I>3\sigma(I)$)	10534
no. of parameters refined	989
refinement method	full-matrix least-squares on F^2
R indices $R_w(F^2)$,[a] $R(F^2)$[b]	0.122, 0.193
goodness-of-fit	1.177

[a] $R_w(F^2) = \{\Sigma[w(F_o^2 - F_c^2)^2]/\Sigma[w(F_o^2)^2]\}^{1/2}$, where all single crystal weights were multiplied by $\min(F_o/F_c, F_c/F_o)$.[4] [b] $R(F^2) = \Sigma|F_o^2 - F_c^2|/\Sigma|F_o^2|$.

Calcd for $Re_2C_{28}H_{48}N_{12}F_2$: C, 34.93; H, 4.99; N, 17.46%. Found: C, 34.73; H, 4.73; N, 17.31%. ^{1}H NMR (C_6D_6, δ): 1.802 (q, $CH_2CH_2CH_2$, 8H), 2.956 (t, CH_2CH_2, 8H), 3.878 (t, CH_2CH_2, 8H).

Synthesis of $[Re_2(hpp)_4F](TFPB)_2$ (4). $Re_2(hpp)_4Cl_2$ (100 mg, 0.100 mmol) and K(TFPB) (182 mg, 0.200 mmol) were mixed together in a 100-mL flask, followed by addition of 15 mL of dichloromethane and 15 mL of ether. A purple solution with suspended white solid which was obtained after stirring overnight was filtered. The purple filtrate was pumped dry, and the solid, presumably $[Re_2(hpp)_4](TFPB)_2$,[40] was used for further reaction. This crude solid (100 mg, 0.0377 mmol) and $[Ag(CH_3CN)_2]PF_6$ (25 mg, 0.0746 mmol) were mixed in a dry box. After addition of 10 mL of dichloromethane, a deep blue color appeared immediately. The mixture was stirred for 15 min and filtered through Celite. The greenish blue filtrate was layered with 30 mL of ether, and block shaped dark blue crystals grew within 1 week. Yield: 53 mg, 53%. IR (KBr, cm^{-1}): 2963 (w), 2876 (w), 1612 (w), 1560 (m), 1479 (w), 1421 (w), 1387 (m), 1352 (m), 1277 (s), 1225 (w), 1127 (s), 1063 (w), 1029 (w), 884 (w), 838 (w), 757 (w), 711 (w), 682 (w). UV−vis (CH_2Cl_2): 424 nm, ϵ = 21 200 L mol^{-1} cm^{-1}, 597 nm, ϵ = 21 900 L mol^{-1} cm^{-1}. Anal. Calcd for $C_{92}H_{72}N_{12}B_2F_{49}Re_2$: C, 41.38; H, 2.72; N, 6.29. Found: C, 41.26; H, 2.57; N, 6.26.

X-ray Crystallography. Single crystals of **1**−**4** were mounted on a nylon cryoloop and transferred to the goniometer of a SMART CCD diffractometer. Data collection and integration were done with the program SMART,[41] and the integrated data were then processed and corrected for Lorentz and polarization effects using the program SAINT.[42] For each compound, an absorption correction was applied using the program SADABS.[43] All structures were solved by the Patterson method and refined by alternate cycles of full-matrix least-squares and difference Fourier maps in the SHELXTL-97 package.[44] Except for the disordered groups found in **1**, **3**, and **4**, non-hydrogen atoms were refined anisotropically, and hydrogen atoms were added at calculated positions and included in the structure factor calculations. Selected bond distances for **1**, **2**·2CH_2Cl_2, **3**·3CH_2Cl_2, and $Re_2(hpp)_4Cl_2$ are listed in Table 1. Crystal data for **1**−**4** are listed in Table 5.

Neutron Data Collection and Refinement. Neutron diffraction data were obtained at the Intense Pulsed Neutron Source (IPNS) at Argonne National Laboratory using the time-of-flight Laue single-crystal diffractometer (SCD).[45,46] At the IPNS, pulses of protons are accelerated into a heavy-element target 30 times a second to produce pulses of neutrons by the spallation process. Exploiting the pulsed nature of the source, neutron wavelengths are determined by time-of-flight based on the de Broglie equation $\lambda = (h/m)\cdot(t/l)$, where h is Planck's constant, m is the neutron mass, and t is the time-of-flight for a flight path l, so that the entire thermal spectrum of neutrons can be used. With two position-sensitive area detectors and a range of neutron wavelengths, a solid volume of reciprocal space is sampled with each stationary orientation of the sample and the detectors. The SCD has two ^{6}Li-glass scintillation position-sensitive area detectors, each with active areas of 15 × 15 cm^2 and a spatial resolution of <1.5 mm. One of the detectors is centered at a scattering angle of 75° and a crystal-to-detector distance of 23 cm, and the second detector is at 120° and 18 cm apart. Details of the data collection and analysis procedures have been published previously.[47]

A single crystal of $[Re_2(hpp)_4F](TFPB)_2$, with approximate dimensions of 5 × 1 × 1 mm and a weight of 9.5 mg, was wrapped in aluminum foil and glued to an aluminum pin that was mounted on the cold stage of a closed-cycle helium refrigerator. The crystal was then cooled to 40 ± 1 K. For each setting of the diffractometer angles, data were stored in three-dimensional histogram form with coordinates x,y,t corresponding to horizontal and vertical detector positions and the time-of-flight, respectively. An auto-indexing algorithm[48] was used to obtain an initial orientation matrix from the peaks in one preliminary histogram measured for 60 min. This unit cell was comparable to the X-ray unit cell indicating that the neutron sample was the correct material. For intensity data collection, runs of 6 h per histogram were used for the data set. Settings were arranged at χ and φ values suitable to cover at least one hemisphere of reciprocal space (Laue symmetry $\bar{1}$). With the above counting times, 22 histograms were completed in the 6 days available for the experiment. Bragg peaks in the recorded histograms were indexed and integrated using individual orientation matrices for each histogram, to allow for any misalignment of the sample. Intensities were integrated about their predicted locations and were corrected for the Lorentz factor, the incident spectrum, and the detector efficiency. A wavelength-dependent spherical absorption

(40) Multiple attempts to isolate single crystals of $[Re_2(hpp)_4](TFPB)_2$ failed. Crystals obtained by diffusion of CH_2Cl_2/hexanes and CH_3CN/ether were twinned.

(41) *SMART, Software for the CCD Detector System, version 5.625*; Bruker Advanced X-ray Solutions: Madison, WI, 2001.
(42) *SAINT. Data Reduction Software. Version 6.33B*; Bruker Advanced X-ray Solutions: Madison, WI, 2001.
(43) *SADABS. Bruker/Siemens Area Detector Absorption and Other Corrections. V2.03*; Bruker Advanced X-ray Solutions: Madison, WI, 2001.
(44) Sheldrick, G. M. *SHELXTL. Version 6.10*; Bruker Advanced X-ray Solutions: Madison, WI, 2000.
(45) Schultz, A. J.; Srinivasan, K.; Teller, R. G.; Williams, J. M.; Lukehart, C. M. *J. Am. Chem. Soc.* **1984**, *106*, 999.
(46) Schultz, A. J. *Trans. Am. Crystallogr. Assoc.* **1987**, *23*, 61.
(47) Schultz, A. J.; Van Derveer, D. G.; Parker, D. W.; Baldwin, J. E. *Acta Crystallogr.* **1990**, *C46*, 276.
(48) Jacobson, R. A. *J. Appl. Crystallogr.* **1976**, *19*, 283.

correction was applied using cross sections from Sears[49] for the non-hydrogen atoms and from Howard et al.[50] for the hydrogen atoms (μ (cm^{-1}) = 1.023 + 0.992 λ). Symmetry related reflections were not averaged since different extinction factors are applicable to reflections measured at different wavelengths.

The GSAS software package was used for structural analysis.[51] The atomic positions from the X-ray diffraction structure were used as a starting point in the refinement. The refinement was based on F^2 values for reflections with a minimum d-spacing of 0.7 Å. Weights were assigned as $w(F_o^2) = 1/[(\sigma(F_o^2) + (F_o^2)]^2$ where σ^2-(F_o^2) is the variance based on counting statistics. In addition, weights were multiplied by a robustness factor $\min(F_o/F_c, F_c/F_o)^4$. In the final refinement, all atoms except the terminal fluorine ligands were refined with isotropic displacement parameters (vide infra). After final refinement the maximum peak of unmodelled scattering density in the difference Fourier map was 1.675 fm Å^{-3} which compares to approximately 33% of the peak height of Re1 in a Fourier map. The minimum peak was −3.765 fm Å^{-3}. These strong difference peaks correspond to atoms already present in the structure that were not modeled anisotropically. Data collection and refinement parameters are summarized in Table 6. Selected bond distances and angles for the cation core of **4** are listed in Table 2.

EPR Spectroscopy. Measurements were performed on both powder and solution/frozen glass samples (10 mM in CH_2Cl_2) between 4 and 340 K and frequencies at 9.4 and 34 GHz using a Bruker E-500 spectrometer system. Microwave power and magnetic field modulation amplitude were adjusted for optimum sensitivity and resolution. The magnetic field was calibrated with digital frequency counters and either an NMR Gaussmeter or the g-marker DPPH (g = 2.0037). W-band measurements were made with a locally developed high-field EPR spectrometer[52] available at the National High Magnetic Field Laboratory at Tallahasse, FL. The magnetic parameters (g-values and hyperfine constants) were determined with the XSophe software package of Bruker employing full matrix diagonalization.

Acknowledgment. We thank the Robert A. Welch Foundation and Texas A&M University for financial support. Helpful discussions with Dr. Dino Villagrán are also acknowledged. Work at Argonne National Laboratory was supported by the U.S. DOE, Basic Energy Sciences−Materials Sciences, under Contract DE-AC-02-06CH11357. The work at Florida State and NHMFL was supported through grants from NSF, DMR-0084173, DMR-0103290, and DMR-0506946 and the State of Florida.

Supporting Information Available: X-ray crystallographic files in CIF format for **1**, **2**·2CH_2Cl_2, **3**·3CH_2Cl_2, and **4** and CIF for the neutron determination of **4**, intensity density maps from the neutron determination, and a figure of the core of the cation in **4** from X-ray data. This material is available free of charge via the Internet at http://pubs.acs.org.

IC062319B

(49) Sears, V. F. In *Methods of Experimental Physics, Vol. 23, Neutron Scattering, Part A*; Academic Press: Orlando, FL, 1986; pp 521−550.
(50) Howard, J. A. K.; Johnson, O.; Schultz, A. J.; Stringer, A. M. *J. Appl. Crystallogr.* **1987**, *20*, 120.
(51) Larson, A. C.; Von Dreele, R. B. *General Structure Analysis System−GSAS*; Los Alamos National Laboratory: Los Alamos, NM, 2000.
(52) Cage, B.; Hassan, A. K.; Pardi, L. A.; Krzystek, J.; Brunel, L. C.; Dalal, N. S. *J. Magn. Reson.* **1997**, *124*, 495.